CHEMISTRY
A EUROPEAN JOURNAL

DOI: 10.1002/chem.200800775

Harnessing a Ratiometric Fluorescence Output from a Sensor Array

Zhuo Wang, Manuel A. Palacios, Grigory Zyryanov, and Pavel Anzenbacher, Jr.*[a]

Abstract: Ratiometric fluorescence-based sensors are widely sought after because they can effectively convert even relatively small changes in optical output into a strong and easy-to-read signal. However, ratiometric sensor molecules are usually difficult to make. We present a proof-of-principle experiment that shows that efficient ratiometric sensing may be achieved by an array of two chromophores, one providing an on-to-off response and the second yielding an off-to-on response in a complementary fashion. In the case that both chromophores emit light of different color, the result is a switching of colors that may be utilized in the same way as from a true ratiometric probe. The chromophore array comprises two sensor elements: i) a polyurethane membrane with embedded *N*-anthracen-9-yl-methyl-*N*-7-nitrobenz-oxa-[1,2,5]diazo-4-yl-*N*′,*N*′-dimethyl-ethylenediamine hydrochloride and ii) a membrane with *N*,*N*-dimethyl-*N*′-(9-methylanthracenyl)ethylenediamine. A combination of photoinduced electron transfer (PET) and fluorescence resonance energy transfer (FRET) allows for green-to-blue emission switching in the presence of Zn^{II} ions. The sensing experiments carried out with different Zn^{II} salts at controlled pH revealed that the degree of color switching in the individual sensor elements depends on both the presence of Zn^{II} ions and the counter anion. These results suggest that sensing of both cations and anions may perhaps be extended to different cation–anion pairs.

Keywords: array · electron transfer · energy transfer · fluorescence · sensors

Introduction

Sensing of metal cations is a focus of numerous studies motivated by human health-related[1] as well as environmental concerns[2] and by the needs for analyses of industrial water streams.[3] Here, the sensors based on metal-induced changes in fluorescence are very attractive as they offer a potential for high sensitivity at a low analyte concentration.[4–6] Fluorescent probes displaying turn-on or ratiometric fluorescence signaling are particularly valuable as this signal transduction is less likely to be biased by nonspecific interactions with background impurities, and offer an improved signal-to-noise ratio.[4,5] Therefore, the design of fluorophores that allow ratiometric sensing is attracting the attention of numerous research groups.

The ratiometric approach circumvents many of the problems of the intensity-based methods, including signal variations due to dye bleaching, fluctuations in source intensity or temperature, and color background of the media.[7] Ratiometric probes and sensor ensembles with a fluorescence output were developed for a number of substrates including pH,[8] alcohol,[9] alkali metal ions,[10] magnesium,[11] calcium,[12] and heavy metals[13] such as cadmium,[14] copper,[15] silver,[16] zinc,[17] carboxylic acids,[18] saccharides,[19] and anions[20] such as phosphates,[21] cyanide[22] and DNA,[23] as well as chemical warfare agents.[24] Of particular interest is the fluorescence and fluorescence-ratiometric sensing of Zn^{II}. This is partly due to the potential utility of such probes in Zn^{II} imaging in biological samples, which is of importance owing to the role of zinc in a variety of physiological functions.[17,25,26]

Ratiometric sensor materials are in many respects unique chromophoric species and their photophysical behavior is often difficult to predict. This may be partly circumvented by a two-chromophore strategy developed for sensing of Zn^{II}, which utilizes two covalently bound chromophores, one of them turned off while the second is turned on in the presence of Zn^{II}, thus generating a different emission output

[a] Dr. Z. Wang, M. A. Palacios, Dr. G. Zyryanov, Prof. P. Anzenbacher, Jr.
Department of Chemistry
and Center for Photochemical Sciences
Bowling Green State University (BGSU)
Bowling Green, OH 43403 (USA)
Fax: (+1) 419-372-9809
E-mail: pavel@bgsu.edu

Supporting information for this article is available on the WWW under http://dx.doi.org/10.1002/chem.200800775: Details of the photophysical properties of **1** and **1**·HCl, crystallographic data for **1** and **1**·HCl, and NMR spectra of **1**, **2**, and **1**·HCl.

WILEY InterScience DISCOVER SOMETHING GREAT
© 2008 Wiley-VCH Verlag GmbH & Co. KGaA, Weinheim

in the presence and absence of Zn^{II} ions.[26f] Recently, ratiometric behavior was also demonstrated in mixtures of two lanthanide luminophores, in which the changes in luminescence correspond to chemical/enzymatic processes, thus generating a ratiometric output independent on a probe concentration. In such probe mixtures the relative intensities of the emission lines can be tuned by adjusting the stoichiometry of the cocktail to obtain a desired information-rich composite luminescence spectrum as a sensor output.[27] A very similar approach was also used to prepare fiber membranes for sensing of dissolved oxygen.[28]

The previous examples of mixture methods, in our opinion, offer a potential change in the paradigm of ratiometric sensing as it applies to the construction of sensor arrays. It is conceivable that for the purpose of fabrication of solid-state array sensors (e.g. using microtiter plates), the cocktail components are placed each in a different well of the array. The information-rich output generally associated with ratiometric sensors may then be effectively obtained numerically from individual sensor elements of the sensor array. This aspect is very important for fabrication of solid-state arrays where the ratiometric mixture may be virtual, derived numerically from the individual components of the virtual ratiometric mixture in separate wells. This is very important because in the solid state or in sensor membranes the components could appear in a close proximity to each other and display undesirable interactions and self-quenching, form exciplexes or ground-state complexes resulting in different luminescence output, etc.[4]

In this study, we show two probes that display a ratiometric output in solution as demonstrated by their fluorescence spectra, and a fluorescence output clearly observable by a naked eye. We identify the structural features responsible for the components of the ratiometric output using fluorescence spectroscopy and X-ray crystallography. Finally, we will show that the fluorescence features observed in the solution are also reflected in the behavior of the sensor array elements fabricated using a polyurethane membrane doped with the individual probes and deposited in a microtiter plate. The sensor performance of such membranes will then be tested using aqueous solutions of Zn^{II} salts. Because even at controlled pH each of the Zn^{II} counter-anions shows a different degree of dissociation, basicity, and so on, the output obtained from the two sensor membranes will comprise the emission-ratiometric output of two different colors of emitted light, but their relative intensity will also be affected by the counter-anion. This may perhaps be later used for determination of salts as cation–anion mixtures.

Results and Discussion

To demonstrate the above principle, we chose *N*-anthracen-9-ylmethyl-*N*-7-nitrobenzoxa[1,2,5]diazol-4-yl-*N*′,*N*′-dimethylethylenediamine (**1**), a recently reported Zn^{II} sensitive fluorescent probe,[29] as the first component of the virtual ratiometric mixture. Compound **1** (see below) can be easily synthesized on a gram scale and purified to photonic-material purity, recrystallized in the form of non-fluorescent monocrystals and its structure determined by X-ray crystallography (see Figure 2). As the second component we chose *N*,*N*-dimethyl-*N*′-(9-methylanthracenyl)ethylenediamine (**2**).

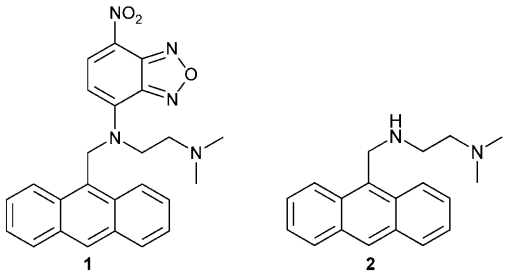

Probe **1** displays only very weak fluorescence ($\Phi \approx 0.001$) for the ANBD-like emission ($\lambda_{exc} = 477$ nm) due to the PET quenching mediated by the dimethylaminoethyl moiety. Similarly, the excitation of the anthracene moiety ($\lambda_{exc} = 350$ nm) does not yield appreciable fluorescence due to the PET/FRET quenching of both the anthracene and 7-nitrobenzoxa[1,2,5]diazole (NBD) moieties. This dark probe does not react to the presence of Zn^{II} salt by appreciable change in fluorescence (Figure 1). Apparently, the presence of Zn^{II} does not preclude the PET quenching by the amine.

We reasoned that since **1** is quenched by the amine-mediated PET, the possibility to make **1** fluorescent is to block the amine-mediated PET, for example, by protonation. Toward this end, we carried out a titration of **1** with $HClO_4$. As expected, the protonation of the amino group results in a dramatic increase in the fluorescence emission from the NBD moiety ($\lambda_{max} = 526$ nm), which is also enhanced by

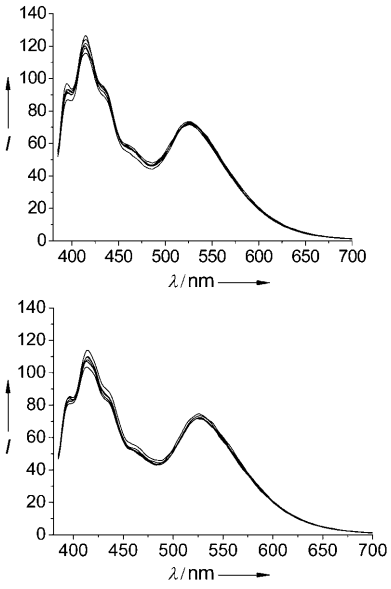

Figure 1. Fluorescence titration of a THF solution of **1** (5 μM) upon addition of 0–10 equiv of Zn^{II} salts, $\lambda_{exc} = 370$ nm. Top: $ZnCl_2$. Bottom: $Zn(AcO)_2$.

 © 2008 Wiley-VCH Verlag GmbH & Co. KGaA, Weinheim

FRET from the anthracene moiety. Again, to confirm the structure of both the non-fluorescent **1** and the fluorescent compound, we prepared the hydrochloride salt of **1** (**1**·HCl). The resulting brightly green fluorescent crystals of **1**·HCl were analyzed spectrally and the structure was unambiguously determined by X-ray crystallography (Figure 2). In the X-ray structure of **1**·HCl, one can clearly see the protonated amine-side chain and the chloride anion coordinated to this proton. The salt **1**·HCl shows an emission maximum at 526 nm corresponding to the NBD moiety.

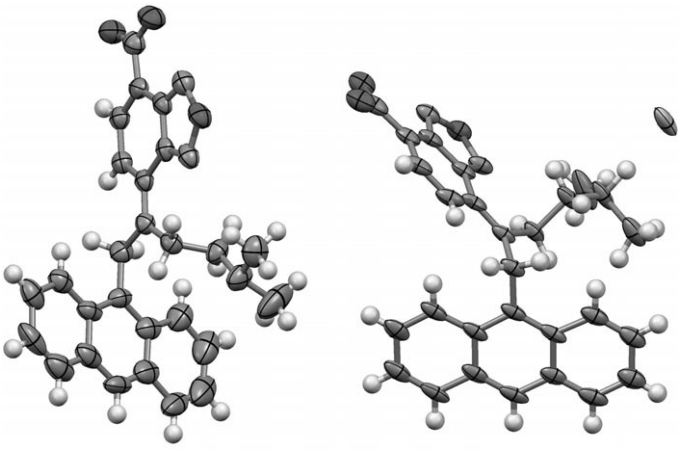

Figure 2. X-ray structure of **1**, and its green fluorescent hydrochloride salt, **1**·HCl. Thermal ellipsoids were scaled to 50% probability level.

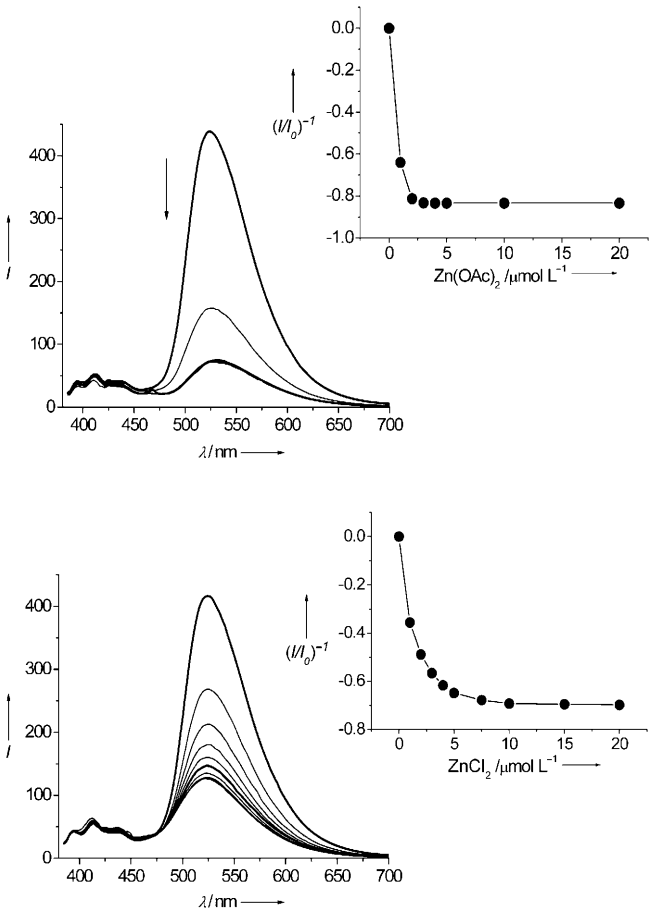

Figure 3. Fluorescence titration of a THF solution of **1**·HCl (5 μM) upon addition of 0–10 equiv of Zn^{II} salts, $\lambda_{exc}=370$ nm, $\lambda_{em}=526$ nm. Top: $Zn(AcO)_2$. Bottom: $ZnCl_2$.

The NBD-based emission at 526 nm of **1**·HCl is quenched in the presence of $ZnCl_2$ or $Zn(AcO)_2$. As presented in Figure 3, **1**·HCl shows quenching saturation after the addition of two equivalents of $ZnCl_2$, while about 0.7–0.9 equivalents suffice for the saturation of the quenching with $Zn(AcO)_2$. The degree of quenching seems to be directly related to the basicity of the counter anion. Furthermore, the final fluorescence spectrum after a quenching process resembles that of a free base **1** (see Figure 1). These observations suggest that the NBD-type fluorescence is quenched largely by anion-mediated deprotonation of **1**·HCl, and that the presence of Zn^{II} does have a relatively small effect in terms of preventing the amine-mediated PET quenching (Figure 3).

N,*N*-Dimethyl-*N*′-(9-methylanthracenyl)ethylenediamine (**2**) was selected as the second component of the sensor because this probe does not show appreciable emission due to the efficient PET quenching of the anthracene fluorophore by the amino residues. However, both aliphatic amine moieties of **2** are capable of coordinating Zn^{II} in a process accompanied by two orders of a magnitude increase of fluorescence intensity (PL $\lambda_{max}=413$ nm, **2**: $\Phi \approx 0.002$; **2**·Zn: $\Phi \approx 0.265$ in THF).[30]

After careful examination of the data, we realized that the desired ratiometric response of the probe mixture **1**·HCl and **2** is a about 200:1 ratio. In such a dilute mixture of **1**·HCl and **2** the intermolecular PET does not readily take place (10^{-5} M). To demonstrate the photophysical properties of such a system, we prepared a solution containing both compounds (**1**·HCl 5 μM and **2**) in a 200:1 ratio. The changes in the fluorescence spectra were recorded after addition of $ZnCl_2$ and $Zn(AcO)_2$ (Figure 4). From the titrations it is clear that the ratiometric behavior of the system depends to a large extent on the counter anion basicity. While the chloride salt quenches the signal from **1**·HCl after addition of ≈20 equiv, the acetate salt quenches **1**·HCl after the addition of only 1–2 equivalents.

These changes in fluorescence upon addition of Zn^{2+} salts may be observed by naked eye (Figure 5). Finally, the mechanism proposed for the ratiometric signalling of the mixture of green fluorescent **1**·HCl and non-fluorescent **2** is summarized in Figure 5 (bottom). In organic solution the chloride provided by $ZnCl_2$ is basic enough to shift the equilibrium towards the formation of **1** (quenched species) while the Zn^{2+} is coordinated by **2** to form a blue fluorescent complex.

The cocktail of mixed sensors with a ratiometric output was found to operate quite well in solution. However, their behavior in the polymer film is often modulated due to the close proximity of both probes in the film. For example,

 © 2008 Wiley-VCH Verlag GmbH & Co. KGaA, Weinheim

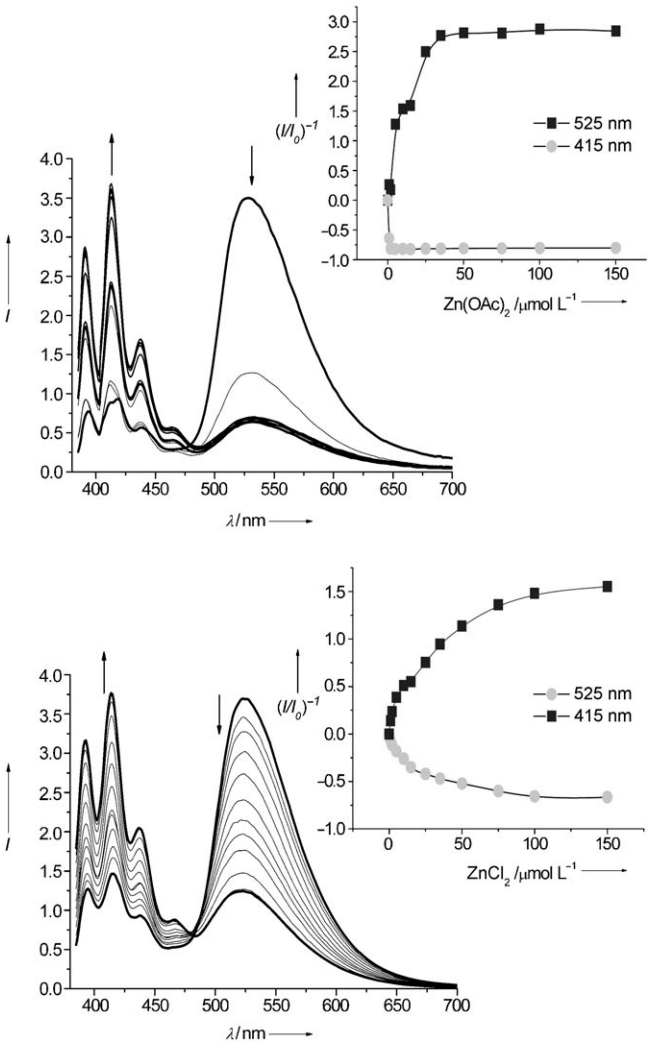

Figure 4. Fluorescence titration of a THF solution of a mixture of **1**·HCl (5 μM) and **2** in a 200:1 molar ratio, $\lambda_{exc}=370$ nm. Top: $Zn(AcO)_2$; Bottom: $ZnCl_2$.

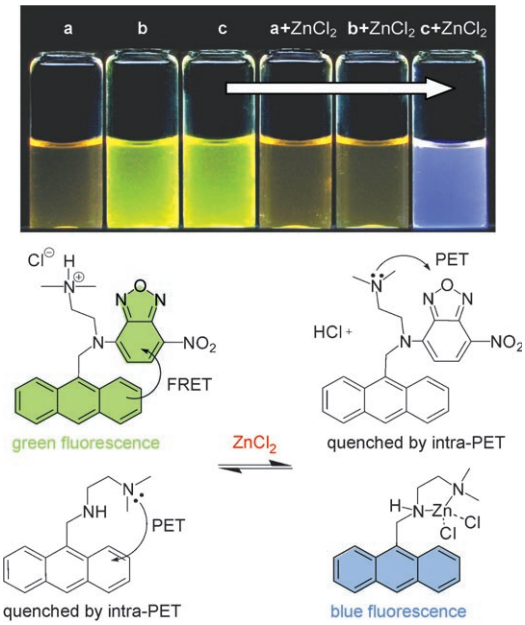

Figure 5. Top: Visualization of changes in the emission of a) **1**, b) **1**·HCl, and c) **1**·HCl (100 μM) + **2** (200:1), upon addition of 20 equiv of $ZnCl_2$. The excitation was carried out with broad band UV excitation $\lambda_{max}=365$ nm. Bottom: A proposed mechanism for the observed ratiometric response.

blue fluorescent **2**·$ZnCl_2$ when in the close proximity of **1** or **1**·HCl may become an effective FRET donor for any of these species, which would result in quenched fluorescence or quenched blue and increased green NBD emission, respectively. In any case, the desired ratiometric output could easily be compromised and would quite likely depend on the concentration of the probes in the polymer film, thus potentially hampering the quality ratiometric action of such sensor film.

For the reasons above, we pursued the virtual ratiometric arrangement, where each of the two sensor membranes comprising probes **1**·HCl and **2** are deposited in separate wells of the microtiter plates. The ratiometric signal may then be "synthesized" numerically and used in the same way the two isotherms (blue for anthracene and green for NBD) were recorded using the probe mixtures (Figure 5). The important difference is that one does not risk potential undesirable interactions between the two probes in the polymer film. To prove this point, we fabricated a simple two-member array using **1**·HCl and **2** dispersed in polyurethane in THF and solution-cast into micro-well plates (Figure 6). Zinc salts water solutions (pH 6.1) were then added to the dry polymer in the wells. The hydrophilic polyurethane serves as a support for the probes and to draw the aqueous analyte into the film and into the close proximity of probes dispersed in the polyurethane material. Seven zinc salts were tested in the array. In the case of a sensor film comprising **1**·HCl, the green NBD fluorescence is quenched presumably due to the deprotonation by counter anions of zinc salts. In agreement with this hypothesis, the salts of less basic anions such as ClO_4^-, Cl^-, SO_4^{2-}, and NO_3^- showed a lower degree of quenching while the more basic anions such as AcO^- and CF_3COO^- displayed stronger quenching of **1**·HCl. In the case of a film comprising a probe **2**, the blue fluorescence is turned on due to the formation of the complex of **2** with zinc (**2**·$ZnCl_2$, the mechanism is shown in Figure 5). The net fluorescence response of the compounds **2** and **1**·HCl with zinc salts is a change from green to blue (Figure 6).

Figure 6 shows that, compared to the control, the **1**·HCl films exposed to Zn^{II} salts give a varying degree of quenching of the green NBD emission. Also, the films with a probe **2** show a dramatic increase in the blue emission upon addition of Zn^{II} salts. Both these features are even clearer from the integrated light intensities in blue and green channel, Figure 6B and C. Figure 6B displays the blue emission, which shows that only blue light is emitted from compound **2**, and that, compared to the control, the films exposed to

 © 2008 Wiley-VCH Verlag GmbH & Co. KGaA, Weinheim

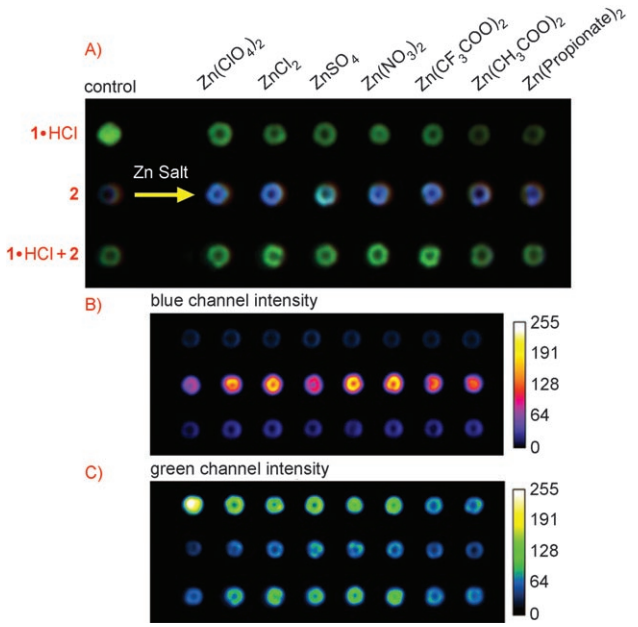

Figure 6. Fluorescent array patterns: A) Micro-wells with sensors **1**·HCl show decreasing intensity of the green emission of **1**·HCl in the presence of Zn^{II} salts and increased intensity in the blue emission of **2**. The **1**·HCl+**2** mixture shows mainly green emission suggesting FRET from **2** to **1**·HCl, which results in a loss of the ratiometric behavior. B) 8-bit Image of the blue channel intensity shows that blue emission appeared chiefly in probe **2** wells. C) 8-bit Image of the green channel intensity shows decrease in the emission of **1**·HCl and a FRET in the **1**·HCl+**2** mixture where the blue emission is absorbed by **1**·HCl and emitted as a green light. Zn^{II} salt solutions: 5 mM, 200 nL, pH 6.1±0.2.

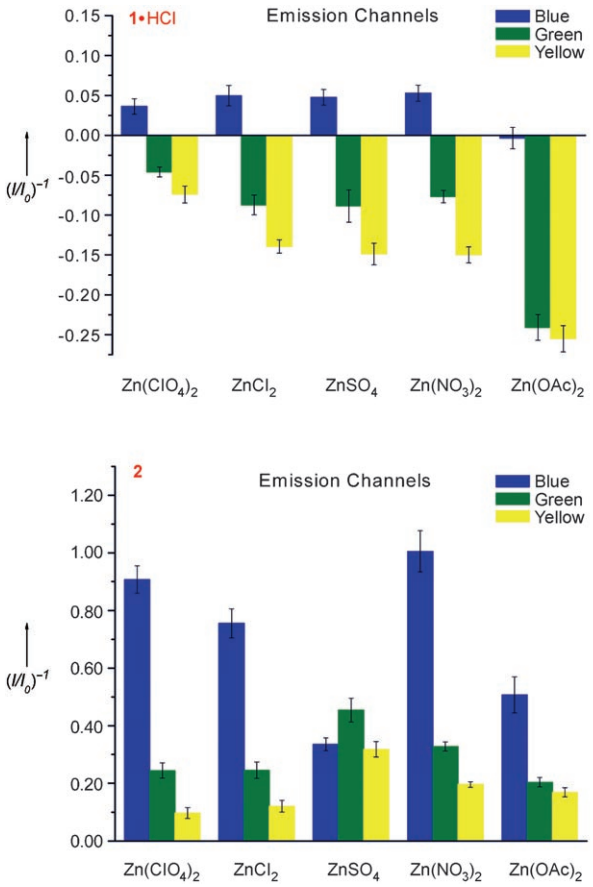

Figure 7. Top: BGY response pattern generated by **1**·HCl upon addition of zinc salts. Bottom: BGY response pattern generated by **2** upon addition of zinc salts. Zn^{II} salt samples: 200 nL, 5 mM, pH 6.1±0.2.

Zn^{II} salts display a strong increase in blue emission. This behavior is consistent with the observation of the behavior in solution described in Figures 4 and 5.

To illustrate the point that the cocktails or solid-state mixtures may not display the ratiometric behavior observed in solution, we included into the array also a polymer doped with a mixture of **1**·HCl and **2**. The Figure 6A shows only green emission and the blue channel (Figure 6B) does not show appreciable blue emission from the solid-state mixture. The green channel (Figure 6C) shows only weak green emission. This suggests possible PET quenching of the NBD emission by the amine of **2** as well as FRET from the **2**·$ZnCl_2$ to the NBD moiety of **1**·HCl. Most importantly, the ratiometric behavior was not observed in the mixture.

The above observation suggested that the sensor films may also be useful in co-determination of counter-anion of the Zn^{II} salt. To investigate the effect of an anion, we used the digital output of the 12-bit CCD camera.[31] The actual responses of the array films were analyzed by recording the amount of light in three channels (blue, green, and yellow, BGY) and compared to the corresponding control (a film without addition of a Zn^{II} salt). The BGY patterns of compound **2** and **1**·HCl were shown in Figure 7. The BGY patterns clearly show that despite the salts having the same pH (pH≈6.1), the anions contribute to different fluorescence output.

The integrated pixel intensities in the BGY channels recorded for various Zn^{II} salts (Figure 7) confirm a varying intensity in the green versus blue channel that could be used to construct the desirable information-rich ratiometric output.[27] Interestingly, different anions yielded a different degree of green-quenching versus blue-increase. This may be due to the several factors including anion basicity, cation–anion dissociation and relative hydrophilicity of anions may be modulating the overall response of the sensor films. It is, however, conceivable that this feature could be used for future identification of salts using both cation and anion contributions. This feature will be a matter of further studies in our laboratory.

Conclusion

In summary, we present a method for generating a virtual ratiometric output from two fluorescent probes displaying turn-off and turn-on signals in the presence of Zn^{II} ions. While the classical ratiometric single molecule probes performing this task are quite rare and difficult to design, the cocktail method using a mixture of two probes, each providing one type of a signal (turn-off or turn-on) is a powerful

 © 2008 Wiley-VCH Verlag GmbH & Co. KGaA, Weinheim

tool allowing to generate a ratiometric output, which even though it is not generated by a single species has most of the qualities of the typical single-molecule ratiometric probes. However, this mixture or a cocktail method often fails in the solid state sensors and arrays where the ratiometric quality of the cocktail signal is compromised by competing photophysical processes. We show that for the purpose of sensor micro-arrays utilizing solid or semi-solid sensor films it is better to use each probe independently and synthesize the ratiometric signal numerically. This simple method, demonstrated here on the example of Zn^{II} salts allows for better predictability and control of the obtained output from the array. Ability to design sensor arrays with predictable behavior of sensor elements is essential for rational design of arrays, which will make it possible to decrease the number of sensor elements without compromising their analytical performance. Last but not least, most likely due to the limited number of intermolecular photophysical processes the separated sensors display analyte specific changes to counter anions, which may allow analyzing metal-anion salts. In part due to its simplicity, we believe this approach is general and will contribute to the design and development of sensor arrays with improved analytical performance in the near future.

Experimental Section

General: Commercially available solvents and reagents were used as received from the chemical suppliers. All reactions were monitored using Whatman K6F Silica Gel 60 Å analytical TLC plates by UV detection (254 and 365 nm). Silica gel (60 Å, 32–63 μm) from EMD Science was used for column chromatography. Melting points (uncorrected) were measured using Hoover capillary melting point apparatus. ^{1}H and ^{13}C APT NMR spectra were recorded using either a Varian spectrometer with working frequency 400 MHz or a Bruker instrument (300 MHz). Chemical shifts were referenced to the residual resonance signal of the solvent. MALDI-TOF/MS were recorded using a Bruker Omniflex spectrometer. GC-MS was recorded using Shimadzu GCMS-QP5050.

Absorption spectra were recorded using a Hitachi U-3010 spectrophotometer. Fluorescence measurements were performed on a single photon counting fluorimeter (Edinburgh Analytical FL/FS 920). Optically dilute solutions used for all photophysical experiments were prepared using spectroscopic grade solvents. For titration experiments the samples were excited at the isosbestic point.

***N*-Anthracen-9-ylmethyl-*N*-7-nitrobenzoxa[1,2,5]diazol-4-yl-*N*′,*N*′-dimethylethylenediamine (1) and *N*,*N*-dimethyl-*N*′-(9-methylanthracenyl)ethylenediamine (2)**: 9-Formylathracene (0.52 g, 2.52 mmol) and N, N-dimethylethylendiamine (0.30 mL, 2.77 mmol) were taken in ethanol and the reaction mixture was stirred for 36 h at room temperature. The Schiff base formed was not isolated. An excess of $NaBH_4$ (0.48 g, 12.50 mmol) was added, and the mixture was refluxed for 4 h. The pale yellow solid remained after removal of the solvent under reduced pressure. Water was added to the flask, and the desired product was extracted with CH_2Cl_2. The combined organic phase was dried by anhydrous Na_2SO_4, and evaporated to yield **2** as yellow oil (0.67 g, 96 %).

Compound **2** (0.65 g, 2.33 mmol) and anhydrous K_2CO_3 (0.35 g, 2.56 mmol) were taken in ethyl acetate and the mixture was stirred for 30 min. The solution was then cooled to 0 °C and subsequently a solution of NBD chloride dissolved in ethyl acetate was added drop-wise with continued stirring for 2 h maintaining the temperature at 0–5 °C. The reaction mixture was then brought to room temperature and stirred for another 2 h to ensure the completion of the reaction. Subsequently, the solvent was evaporated under vacuum and the residue was purified by column chromatography (silica gel) with EtOAc/hexanes 3:1. The orange yellow powder **1** was obtained finally. (Conversion 60 % after chromatographic column the yield is 16.6 %.)

Characterization of 1: m.p. 207–209 °C; ^{1}H NMR (300 MHz, $CDCl_3$, 25 °C, TMS): $\delta = 1.725$ (s, 6H), 2.171 (t, $J = 7.2$ Hz, 2H), 3.682 (t, $J = 7.2$ Hz, 2H), 6.106 (s, 2H), 6.601 (d, $J = 9$ Hz, 1H), 7.528–7.604 (m, 4H), 8.084–8.142 (m, 4H), 8.605 ppm (m, 2H); ^{1}H NMR (400 MHz, $CDCl_3$, 25 °C, TMS): $\delta = 1.717$ (s, 6H), 2.161 (t, $J = 7.2$ Hz, 2H), 3.667 (t, $J = 7.2$ Hz, 2H), 6.079 (s, 2H), 6.577 (d, $J = 9$ Hz, 1H,), 7.525–7.589 (m, 4H), 8.077–8.123 (m, 4H), 8.585 ppm (m, 2H); ^{13}C ATP NMR: (75 MHz, $CDCl_3$, 25 °C, TMS): $\delta = 45.20$ (CH_3), 47.63 (CH_2), 49.10 (CH_2), 56.46 (CH_2), 102.18 (CH), 123.13 (CH), 123.28 (C), 124.02 (C), 125.44 (CH), 127.57 (CH), 129.69 (CH), 129.87 (CH), 131.40 (C), 131.65 (C), 135.34 (CH), 145.05 (C), 145.20 (C), 145.56 ppm (C); MALDI-MS: *m*/*z*: calcd for: 441.18; found: 441.13 [M^+].

Characterization of 2: ^{1}H NMR (300 MHz, $CDCl_3$, 25 °C, TMS): $\delta = 2.187$ (s, 6H), 2.481 (t, $J = 6$ Hz, 2H), 2.950 (t, $J = 6$ Hz, 2H), 4.752 (s, 2H), 7.260–7.561 (m, 4H), 7.990–8.022 (m, 2H), 8.350–8.353 ppm (m, 2H); ^{13}C NMR (75 MHz, $CDCl_3$, 25 °C, TMS): $\delta = 45.50$ (CH_3), 45.79 (CH_2), 47.77 (CH_2), 58.99 (CH_2), 124.34 (CH), 124.93 (CH), 126.04 (CH), 127.16 (C), 129.18 (CH), 130.44 (C), 131.62 (CH), 131.96 ppm (C); MALDI-MS: *m*/*z*: calcd for: 278.18; found: 278.13 [M^+].

Characterization of 1·HCl: m.p. 196–198 °C; ^{1}H NMR (300 MHz, $CDCl_3$, 25 °C, TMS): $\delta = 2.030$ (s, 6H), 2.492 (t, $J = 7.2$ Hz, 2H), 4.108 (t, $J = 7.2$ Hz, 2H), 6.210(s, 2H), 6.978 (d, $J = 9$ Hz, 1H), 7.585–7.661 (m, 4H), 8.090–8.131 (m, 4H), 8.632–8.665 ppm (m, 2H); ^{13}C NMR (75 MHz, DMSO-d_6, 25 °C): 42.53(CH_3), 43.59 (CH_2), 48.52 (CH_2), 53.36 (CH_2), 105.54 (CH), 118.52 (C), 123.50 (C), 124.01 (CH), 124.89 (C), 126.05 (CH), 127.23 (C), 128.20 (CH), 129.98 (CH), 130.16 (CH), 131.47 (C), 131.70 (C), 136.78 (CH), 145.26 (C), 145.65 (C), 145.81 ppm (C); MALDI-MS: *m*/*z*: calcd for: 477.16; found: 442.23 [$M-Cl$]$^+$.

Sensor arrays: The array chips were fabricated by ultrasonic drilling of microscope slides (μ-well diameter: 500 ± 10 μm, depth: 500 ± 10 μm). The wells were filled with 200 nL (approx. 0.08 % sensor in polyurethane, w/w) in a Tecophilic THF solution (4 % w/w) and dried to form a 5 μm thick polymer film in each well. In a typical assay, the zinc salts were added as aqueous solutions (200 nL, 5 mM, pH 6.1 ± 0.2). Images from the arrays were recorded using a Kodak Image Station 440CF. The sensor arrays were excited with a broadband UV lamp (300–400 nm, $\lambda_{max} = 365$ nm) and an emission intensity in three channels was utilized for signal output using the following filters: (**B**) Blue: band-pass filter 380–500 nm $\lambda_{max} = 435$ nm (**G**) Green: band pass filter 480–600 nm $\lambda_{max} = 525$ nm (**Y**) Yellow: long pass filter 523 nm. After acquiring the images, the integrated (non zero) grey pixel (n) value is calculated for each well of each channel. Images of the sensor chip were recorded before (b) and after (a) the addition of analyte and their relative intensities (R) were calculated as follows:

$$R = \sum_n \frac{a_n}{b_n} - 1$$

The gray pixel value is a numerical value of the grey shade that for a 12-bit pixel depth detector ranges between 0–4095.

Acknowledgements

Financial support from the Alfred Sloan Foundation, BGSU (Technology Innovations Enhancement grant), and the NSF (CHE-0750303, EXP-LA 0731153). M.A.P. acknowledges support from the McMaster Endowment.

[1] L. Jaerup, *Br. Med. Bull.* **2003**, *68*, 167–182.
[2] V. Mani, H. Kaur, M. Mohini, *J. Ind. Pollut. Control* **2005**, *21*, 101–107.

 © 2008 Wiley-VCH Verlag GmbH & Co. KGaA, Weinheim

[3] L. K. Wang, *Treatment of power industry wastes. Waste Treatment in the Process Industries* (Ed.: L. K. Wang), CRC Press LLC, Boca Raton, **2006**, pp. 581–621.
[4] J. R. Lakowicz *Principles of Fluorescence Spectroscopy*, 3rd ed., Springer, New York, **2006**.
[5] Advanced Concepts in Fluorescence Sensing. Small Molecule Sensing in *Top. Fluoresc. Spectrosc. Vol. 9* (Eds: C. D. Geddes, J. R. Lakowicz), Springer Science, New York, **2005**.
[6] a) E. V. Anslyn, *J. Org. Chem.* **2007**, *72*, 687–699; b) B. Valeur, I. Leray, *Coord. Chem. Rev.* **2000**, *205*, 3–40; c) A. P. de Silva, H. Q. N. Gunaratne, T. Gunnlaugsson, A. J. M. Huxley, C. P. McCoy, J. T. Rademacher, T. E. Rice, *Chem. Rev.* **1997**, *97*, 1515–1566; d) J. F. Callan, A. P. de Silva, D. C. Magri, *Tetrahedron* **2005**, *61*, 8551–8588.
[7] Advanced Concepts in Fluorescence Spectroscopy, Part B in *Top. Fluoresc. Spectrosc. Vol. 10* (Eds: C. D. Geddes, J. R. Lakowicz), Springer, New York, **2005**.
[8] H. R. Kermis, Y. Kostov, P. Harms, G. Rao, *Biotechnol. Prog.* **2002**, *18*, 1047–1053.
[9] S. Petrova, Y. Kostov, K. Jeffris, G. Rao, *Anal. Lett.* **2007**, *40*, 715–727.
[10] N. B. Sankaran, S. Nishizawa, M. Watanabe, T. Uchida, N. Teramae, *J. Mater. Chem.* **2005**, *15*, 2755–2761.
[11] E. J. Park, M. Brasuel, C. Behrend, M. A. Philbert, R. Kopelman, *Anal. Chem.* **2003**, *75*, 3784–3791.
[12] A. Coskun, E. Deniz, E. U. Akkaya, *J. Mater. Chem.* **2005**, *15*, 2908–2912.
[13] M. A. Palacios, Z. Wang, V. A. Montes, G. V. Zyryanov, B. J. Hausch, K. Jursikova, P. Anzenbacher Jr. , *Chem. Commun.* **2007**, 3708–3710.
[14] C. Lu, Z. Xu, J. Cui, R. Zhang, X. Qian, *J. Org. Chem.* **2007**, *72*, 3554–3557.
[15] M. Royzen, Z. Dai, J. W. Canary, *J. Am. Chem. Soc.* **2005**, *127*, 1612–1613.
[16] A. Coskun, E. U. Akkaya, *J. Am. Chem. Soc.* **2005**, *127*, 10464–10465.
[17] a) P. Carol, S. Sreejith, A. Ajayaghosh, *Chem. Asian J.* **2007**, *2*, 338–348; b) C. J. Chang, S. J. Lippard, *Metal Ions in Life Sciences* **2006**, *1* (Neurodegenerative Diseases and Metal Ions), 321–370; c) C. J. Chang, J. Jaworski, E. M. Nolan, M. Sheng, S. J. Lippard, *Proc. Natl. Acad. Sci. USA* **2004**, *101*, 1129–1134.
[18] F. Galindoa, J. Becerrila, M. I. Burguetea, S. V. Luis, L. Vigara, *Tetrahedron Lett.* **2004**, *45*, 1659–1662.
[19] R. Ozawa, T. Hayashita, T. Matsui, C. Nakayama, A. Yamauchi, I. Suzuki, *J. Inclusion Phenom. Macrocyclic Chem.* **2008**, *60*, 253–261.
[20] F. Oton, A. Tarraga, P. Molina, *Org. Lett.* **2006**, *8*, 2107–2110.
[21] a) X. Peng, Y. Xu, S. Sun, Y. Wu, J. Fan, *Org. Biomol. Chem.* **2007**, *5*, 226–228; b) A. Ojida, H. Nanaka, Y. Miyahara, S. Tamaru, K. Sada, I. Hamachi, *Angew. Chem.* **2006**, *118*, 5644–5647; *Angew. Chem. Int. Ed.* **2006**, *45*, 5518–5521.
[22] R. Badugu, J. R. Lakowicz, C. D. Geddes, *J. Am. Chem. Soc.* **2005**, *127*, 3635–3641.
[23] A. A. Marti, S. Jockusch, N. Stevens, J. Ju, N. J. Turro, *Acc. Chem. Res.* **2007**, *40*, 402–409.
[24] S.-W. Zhang, T. M. Swager, *J. Am. Chem. Soc.* **2003**, *125*, 3420–3421.
[25] N. C. Lim, H. C. Freake, C. Brückner, *Chem. Eur. J.* **2005**, *11*, 38–49.
[26] a) K. Komatsu, Y. Urano, H. Kojima, T. Nagano, *J. Am. Chem. Soc.* **2007**, *129*, 13447–13454; b) S. Sumalekshmy, M. M. Henary, N. Siegel, P. V. Lawson, Y. Wu, K. Schmidt, J.-L. Bredas, J. W. Perry, C. J. Fahrni, *J. Am. Chem. Soc.* **2007**, *129*, 11888–11889; c) E. M. W. M. van Dongen, L. M. Dekkers, K. Spijker, E. W. Meijer, L. W. J. Klomp, M. Merkx, *J. Am. Chem. Soc.* **2006**, *128*, 10754–10762; d) M. Taki, J. L. Wolford, T. V. O'Halloran, *J. Am. Chem. Soc.* **2004**, *126*, 712–713; e) C. C. Woodroofe, A. C. Won, S. J. Lippard, *Inorg. Chem.* **2005**, *44*, 3112–3120; f) C. C. Woodroofe, S. J. Lippard, *J. Am. Chem. Soc.* **2003**, *125*, 11458–11459; g) S. Maruyama, K. Kikuchi, T. Hirano, Y. Urano, T. Nagano, *J. Am. Chem. Soc.*, **2002**, 124, 10650–10651.
[27] M. S. Tremblay, M. Halim, D. Sames, *J. Am. Chem. Soc.* **2007**, *129*, 7570–7577.
[28] E. J. Park, K. R. Reid, W. Tang, R. T. Kennedy, R. Kopelman, *J. Mater. Chem.* **2005**, *15*, 2913–2919.
[29] S. Banthia, A. Samanta, *J. Phys. Chem. B* **2006**, *110*, 6437–6440.
[30] B. Bag, P. K. Bharadwaj, *J. Phys. Chem. B* **2005**, *109*, 4377–4390.
[31] Because the graphic outputs are 8-bit images (Figure 7) obtained by conversion from the 12-bit signal their dynamic range is lower.

Received: April 24, 2008
Published online: August 7, 2008

 © 2008 Wiley-VCH Verlag GmbH & Co. KGaA, Weinheim